Steric effects in the design of Co-Schiff base complexes for the catalytic oxidation of lignin models to *para*-benzoquinones†

Berenger Biannic,[a] Joseph J. Bozell*[a] and Thomas Elder[b]

New Co-Schiff base complexes that incorporate a sterically hindered ligand and an intramolecular bulky piperazine base in close proximity to the Co center are synthesized. Their utility as catalysts for the oxidation of *para*-substituted lignin model phenols with molecular oxygen is examined. Syringyl and guaiacyl alcohol, as models of S and G units in lignin, are oxidized in good yield using a catalyst bearing an *N*-benzylpiperazinyl substituent, with the catalysts displaying improved reactivity for G oxidation. Computational evaluation of the catalysts shows that the piperazinyl substituent is within bonding distance of the Co center. The increased steric interference is suggested as the source of increased G reactivity.

Introduction

By using renewable carbon (biomass) as a raw material, the integrated biorefinery is emerging as an alternative to the petrochemical refinery for the simultaneous production of biobased chemicals and fuels. Central to the viability of this new industry will be its capacity to transform each of the primary components of biomass into biobased products.[1] Lignin offers both opportunity and challenge in this regard, as it can be nearly 25% of lignocellulosic biomass, making it the second most abundant source of renewable carbon in the biosphere, and the most likely source of biobased aromatics.[2] However, lignin possesses a highly heterogeneous polyaromatic structure. Heterogeneity is introduced during a biosynthetic process that couples delocalized phenoxy radicals formed from a small group of primary monolignols (Fig. 1), leading to a variety of different substructural units.[3] Lignin from woody feedstocks is constructed mostly from syringyl (S) and guaiacyl (G) units derived from sinapyl and coniferyl alcohol, respectively. Herbaceous feedstocks (grasses) incorporate *p*-hydroxyphenyl (H) units into the lignin polymer as well as coumaric and ferulic acid as end caps and crosslinkers.[4] Moreover, the structure of lignin as found in nature changes, often dramatically, during processes used for its isolation within the bio-
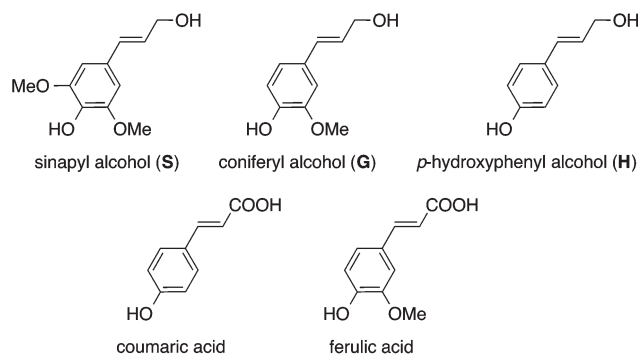

Fig. 1 Monolignol units used in the biosynthesis of the lignin biopolymer.

refinery.[5] Effective use of lignin therefore requires processes able to accommodate all of the various substructural units present within the raw material.

The electron rich nature of the aromatic units in lignin suggests that they should be subject to selective oxidation. Indeed, the pulp and paper industry practices *nonselective* oxidation of lignin on a massive scale for the purposes of lignin removal from cellulose pulp.[6] Recent reports describe new oxidative methodology for transforming lignin models into low molecular weight aromatics using reductive processes catalyzed by Ru,[7] Ni[8] and Pd,[9] oxidative and non-oxidative processes catalyzed by Co[10] and V,[11] or organocatalytic processes using TEMPO.[12] These studies focus almost exclusively on the cleavage of dimeric, non-phenolic β-aryl ether models, representative of lignin's β-O-4 linkage, which can account for 50–65% of the substructural units present in native lignin. Unfortunately, a focus on this linkage may not provide an appropriate representation of the lignin actually available for

[a]*Center for Renewable Carbon, Center for the Catalytic Conversion of Biomass (C3Bio), 2506 Jacob DriveUniversity of Tennessee, Knoxville, TN 37996, USA. E-mail: jbozell@utk.edu*
[b]*USDA-Forest Service, Southern Research Station, 251 DeVall Drive, Auburn, AL 36849, USA*
†Electronic supplementary information (ESI) available: Synthetic and analytical details for new complexes, computational methodology, minimized structures for complexes **17a**, **17c**, and **17e**. See DOI: 10.1039/c4gc00709c
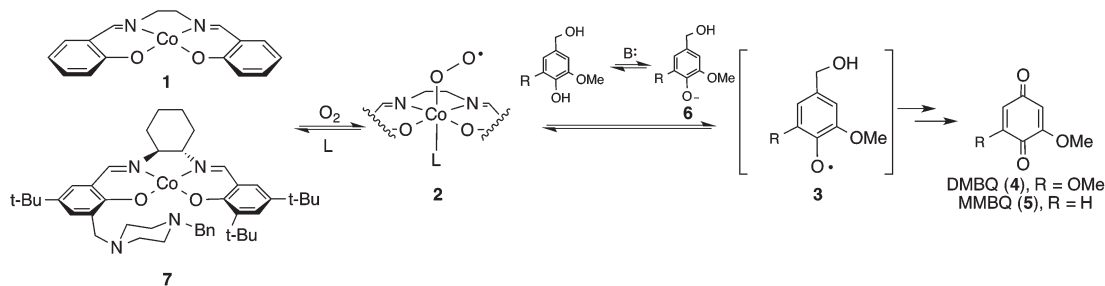
Fig. 2 Initial steps in Co-Schiff base catalyzed oxidation of phenols.

conversion within the biorefinery because leading processes for biomass separation may eliminate β-O-4 units during lignin isolation.[13] Moreover, as these β-O-4 units are lost, there is a concomitant increase in free phenolic hydroxyl functionality.[14] Thus, catalytic processes targeting conversion of lignin-like phenols would provide a more realistic probe of lignin as a chemical feedstock.

Co-Schiff base complexes catalyze the aerobic oxidation of phenols under mild conditions (Fig. 2). In the presence of an external ligand such as pyridine, the Co catalysts [*e.g.*, Co(salen), **1**] bind molecular oxygen to form a Co-superoxo complex **2**.[15] With simple Co-Schiff base complexes, formation of **2** is significantly improved by addition of pyridine as an external axial ligand because **1** itself binds oxygen poorly.[16] The resulting complex **2** abstracts a phenolic hydrogen from the substrate to generate phenoxy radical **3**, initiating a process that affords production of *para*-benzoquinones from *para*-substituted lignin model phenols. We reported some of the first examples of this transformation by converting S lignin models to dimethoxybenzoquinone (DMBQ, **4**) and G lignin models to monomethoxybenzoquinone (MMBQ, **5**).[17] Although the oxidation proceeds in good yield for the production of **4**, catalyst **1** gives low yields of **5** from oxidation of G model phenols. However, the yield of **5** from G models is improved when the reaction is supplemented with a sterically hindered, non-coordinating aliphatic base, such as DIPEA.[18]

Recently, we reported that appending the hindered base to an aromatic ring of the Schiff-base ligand (*e.g.*, complex **7**) markedly improves yields, reaction times and catalyst loadings for the oxidation of both S and G model monomers and dimers in the absence of an added external ligand.[19] The results suggest that the presence of a bulky aliphatic base bound in close proximity to the Co-superoxo complex promotes the formation of the phenoxy radical **3** through formation of an easily oxidized phenoxide intermediate **6**. Parallel computational results on the reactivity of **1** in the presence of a series of substituted imidazoles as axial bases further suggest that the steric environment around the Co influences the geometry and reactivity of **2**.[20]

Based on these results, we wished to examine how synthetic design of the steric and electronic environment about the Co center in second-generation oxidation catalysts such as **7** could be exploited to optimize the reactivity of the complex. We report the synthesis and reactivity of a new family of unsymmetrical

Co-Schiff base complexes bearing hindered, aliphatic nitrogen bases on the ligand's ethylenediamine bridge as well as their use as catalysts for oxidation of primary lignin models in the presence of molecular oxygen. We further present preliminary computational results regarding the effect of the intramolecular base near the Co center and its impact on the mechanism of oxidation.

Experimental

General information

Specific details and analytical data for synthesis of new catalysts are available as ESI.† All reactions were carried out under an atmosphere of nitrogen unless otherwise specified. Anhydrous tetrahydrofuran (THF) was purified by distillation over sodium/benzophenone. All reagents and solvents were purchased from commercial sources and were used as received. Analytical thin layer chromatography (TLC) was performed using 250 μm Silica Gel 60 F254 pre-coated plates. Flash column chromatography was performed using 230–400 mesh 60 Å silica gel. The eluents employed are reported as volume : volume percentages. Melting points were recorded on a Fisher-Johns melting point apparatus and are uncorrected. Catalytic oxidations were carried out in thick walled glass reactors under the oxygen pressure indicated in the text. ^{1}H and ^{13}C NMR spectra were measured in CDCl$_3$ using a Varian Unity 400 MHz instrument. Chemical shifts are reported relative to tetramethylsilane or solvent resonance and reported in ppm. Infrared spectra were obtained on a Perkin-Elmer Spectrum One FT-IR spectrometer at 4 cm^{-1} resolution and are reported in cm^{-1}. High resolution mass spectra (HRMS) were obtained by The Center for Mass Spectrometry of the Department of Chemistry at the University of Tennessee, and are reported as *m/z* (relative ratio). Accurate masses are reported for the molecular ion (M + H)$^+$ or a suitable fragment ion and are reported with an error <5 ppm. 1-Octylpiperazine **15b**, 1-methylpiperazine **15c**, 1-phenylpiperazine **15d** and piperidine **15e** were purchased from Sigma-Aldrich and used as received.

2,3-Bis((*E*)-(3,5-di-*tert*-butyl-2-hydroxybenzylidene)amino)-propan-1-ol (13). To a solution of 2,3-dibromopropanol **8** (2.179 g, 10 mmol) in dry DMF (60 mL) was added NaN$_3$ (6.500 g, 100 mmol). The reaction mixture was heated at reflux under N$_2$ for 24 hours (dark brown), cooled to room tempera-

ture and treated with water (100 mL). The crude product was extracted with EtOAc (2 × 100 mL), rinsed with water (2 × 100 mL), dried over Na_2SO_4 and concentrated to afford a mixture of diazide **9** and 2-bromoprop-2-en-1-ol **10**[21] (10/1) as a light brown oil which was used in the next step without further purification; 2,3-diazidopropan-1-ol **9**: ^{1}H-NMR (400 MHz, $CDCl_3$): 3.77–3.62 (m, 3H), 3.47 (dq, J = 18.1, 4.4 Hz, 2H); ^{13}C-NMR (100 MHz, $CDCl_3$): δ 62.8, 62.4, 51.7. When non-dry DMF was used as solvent, 1,3-diazidopropan-2-ol was isolated as the major product: ^{1}H-NMR (400 MHz, $CDCl_3$): 3.95–3.91 (m, 1H), 3.42–3.36 (dd, J = 7.8 Hz, 4H): ^{13}C-NMR (100 MHz, $CDCl_3$): δ 69.8, 54.1.

To a solution of diazide **9** obtained above in THF–H_2O (50 mL, 4/1) was added Ph_3P (5.246 g, 20 mmol) portionwise at room temperature (N_2 evolution was observed). The reaction mixture was heated at reflux overnight, diluted with water (20 mL) and THF was evaporated under vacuum. The mixture was triturated, the white solid formed was filtered, rinsed with H_2O (10 mL) and the aqueous solution was concentrated under vacuum (60 °C) to give 2,3-diaminopropan-1-ol **11** as a yellow oil which was used in the next step without further purification. Presence of residual water or DMF in the crude material does not affect the yield of the next reaction.

To a solution of **11** obtained above in MeOH (50 mL) was added 3,5-di-*tert*-butyl-2-hydroxybenzaldehyde **12** (2.340 g, 10 mmol) in one portion. The reaction mixture was heated at reflux for 6 hours, concentrated under vacuum and the crude material purified by flash chromatography (gradient; 0–50–100% CH_2Cl_2–hexanes) to give **13** as a thick bright yellow oil (2.103 g, 41%) which slowly solidified over time; mp 90–93 °C; R_f = 0.25 (50% CH_2Cl_2–hexanes + 1% Et_3N); IR (neat) 3354, 2953, 2911, 2857, 1626, 1439, 1249, 1172, 877, 730 cm^{-1}; ^{1}H-NMR (400 MHz, $CDCl_3$): δ 13.48 (s, 1H), 13.33 (bs, 1H), 8.45 (s, 1H), 8.36 (s, 1H), 7.38 (d, J = 2.4 Hz, 1H), 7.36 (d. J = 2.4, 1H), 7.09 (d, J = 2.4 Hz, 1H, 7.05 (d, J = 2.4 Hz, 1H), 3.96–3.93 (m, 2H), 3.88–3.83 (m, 1H), 3.76–3.66 (m, 2H), 1.43 (s, 9H), 1.42 (s, 9H), 1.28 (s, 18H); ^{13}C-NMR (100 MHz, $CDCl_3$): δ 168.3, 168.0, 140.4, 140.1, 136.6, 127.4, 127.2, 126.4, 126.1, 117.8, 117.7, 71.6, 64.6, 61.1., 35.0, 34.1, 31.5, 29.5, 29.4; HRMS (DART-TOF) Calcd for $C_{33}H_{50}N_2O_3$ (M + H)$^+$: 523.38997; found 523.38990.

2,3-Bis((*E*)-(3,5-di-*tert*-butyl-2-hydroxybenzylidene)amino)-propyl methanesulfonate (14). To a solution of alcohol **13** (1.000 g, 1.92 mmol) and Et_3N (517 µL, 3.84 mmol) in CH_2Cl_2 (10 mL) was added methanesulfonyl chloride (221 µL, 2.87 mmol) dropwise at 0 °C. The reaction mixture was stirred at the same temperature for 1 hour, quenched by addition of $NaHCO_3$ (20 mL of a saturated aqueous solution) and diluted with CH_2Cl_2 (20 mL). The organic fraction was separated, dried over Na_2SO_4 and concentrated to give **14** as a thick yellow oil (1.094 g, 95%) which slowly solidified over time; mp 166–169 °C; R_f = 0.25 (50% CH_2Cl_2–hexanes + 1% Et_3N); IR (neat) 2959, 2869, 1630, 1439, 1353, 1332, 1180, 996, 979, 826 cm^{-1}; ^{1}H-NMR (400 MHz, $CDCl_3$): δ 13.26 (s, 1H), 13.06 (bs, 1H), 8.46 (s, 1H), 8.38 (s, 1H), 7.40 (d, J = 2.4 Hz, 1H), 7.38 (d. J = 2.4, 1H), 7.09 (d, J = 2.4 Hz, 1H), 7.06 (d, J = 2.4 Hz, 1H),

4.54 (dd, J = 10.8, 4.4 Hz, 1H), 4.43 (dd, J = 10.0, 7.2 Hz, 1H), 3.98–3.79 (m, 3H), 3.01 (s, 3H); 1.43 (s, 9H), 1.42 (s, 9H), 1.28 (s, 18H); ^{13}C-NMR (100 MHz, $CDCl_3$): δ 169.0, 168.8, 157.9, 157.9, 140.5, 140.3, 136.8, 136.7, 127.9, 127.5, 126.6, 126.3, 117.6, 117.5, 70.4, 68.3, 60.8., 37.5, 35.0, 34.1, 34.1, 31.6, 31.4, 31.4, 29.4; HRMS (DART-TOF) Calcd for $C_{34}H_{52}N_2O_5S$ (M + H)$^+$: 601.36752; found 601.36934.

Schiff base 16a. To a solution of mesylate **14** (510.8 mg, 0.85 mmol) in dry MeCN (8 mL) was added successively DIPEA (593 µL, 3.4 mmol), 1-benzylpiperazine **15a**[22] (450.1 mg, 2.55 mmol) and potassium iodide (30.0 mg, 0.18 mmol) at room temperature. The reaction mixture was heated at reflux for 24 hours (dark orange), quenched by addition of water (30 mL) and extracted with CH_2Cl_2 (2 × 50 mL). The organic fractions were combined, dried over Na_2SO_4, concentrated under vacuum and the crude product purified by flash chromatography (gradient; 0–2% MeOH–CH_2Cl_2) to give the product as a thick bright yellow oil (376.3 mg, 65%) which slowly solidified over time; mp 91–93 °C; R_f = 0.10 (100% CH_2Cl_2); IR (neat) 2952, 2866, 2807, 1630, 1460, 1443, 1360, 1252, 1176, 830, 736, 698 cm^{-1}; ^{1}H-NMR (400 MHz, $CDCl_3$): δ 13.68 (bs, 1H), 13.56 (bs, 1H), 8.34 (s, 1H), 8.33 (s, 1H), 7.34–7.04 (m, 7H), 7.04 (d, J = 2.4 Hz, 1H), 7.02 (d, J = 2.4 Hz, 1H), 4.09 (dd, J = 12.0, 2.4 Hz, 1H), 3.75–3.60 (m, 2H), 3.49 (s, 2H), 2.73 (dd, J = 13.2, 6.8 Hz, 1H), 2.60–2.46 (m, 5H), 1.42 (s, 9H), 1.41 (s, 9H), 1.27 (s, 9H), 1.26 (s, 9H); ^{13}C-NMR (100 MHz, $CDCl_3$): δ 167.8, 167.1, 158.3, 158.2, 140.2, 140.2, 138.4, 136.8, 136.7, 129.4, 128.4, 127.2, 127.2, 127.1, 126.4, 126.2, 118.1, 118.0, 67.5, 63.3, 63.0, 62.1, 54.0, 53.4, 35.2, 34.3, 31.7, 29.6; HRMS (DART-TOF) Calcd for $C_{44}H_{64}N_4O_2$ (M + H)$^+$: 681.51075; found 681.50843.

Cobalt-Schiff base complex 17a. To a solution of Schiff base **16a** (121.3 mg, 0.18 mmol) in i-propanol (2 mL) was added a solution of $Co(OAc)_2 \cdot 4H_2O$ (44.3 mg, 0.18 mmol) in methanol (1 mL). The mixture was heated at reflux for 3 h under argon. The dark brown solution was concentrated and the product was precipitated in 15 mL of hexanes. The green brown solid was recovered by filtration, rinsed with hexanes and then dried under vacuum for 16 h at 80 °C to give **17a** (102.1 mg, 78%) as a red/light brown solid. IR (neat) 2952, 2911, 2866, 1595, 1529, 1363, 1315, 1252, 1169, 788, 702 cm^{-1}; HRMS (DART-TOF) Calcd for $C_{44}H_{62}CoN_4O_2$ (M + H)$^+$: 738.42830; found 738.42596.

General procedures for the oxidation of *p*-phenols to benzoquinones

In a Fisher-Porter bottle, *p*-phenol substrate (1 mmol) and Co-Schiff base complex **17a–f** (0.05 mmol) were combined in 5 mL of MeOH or 5 mL of MeOH–CH_2Cl_2 (4/1) for catalyst **22**. The bottle was flushed with oxygen three times and then pressurized with oxygen to 50 psi. After 16 hours under vigorous stirring, the reaction mixture is concentrated under vacuum at room temperature and the crude material purified by flash chromatography (eluent: gradient 0–5–10% EtOAc–CH_2Cl_2). 2,6-Dimethoxybenzoquinone **4** (bright yellow) was recovered by filtration at the end of the reaction and satisfactorily matched

all previously reported data. 2,6-Dimethoxybenzoquinone is only partially soluble in methanol, and between 5 and 10% of residual product remains in solution that can be purified by column chromatography (eluent: gradient 0–5–10% EtOAc–CH$_2$Cl$_2$). When catalyst **22** was used, the reaction mixture was concentrated under vacuum and purified by flash chromatography (eluent: gradient 0–5–10% EtOAc–CH$_2$Cl$_2$). 2-Methoxybenzoquinone **5** (light green) was purified by flash chromatography (eluent: gradient 0–5% EtOAc–CH$_2$Cl$_2$) and satisfactorily matched all previously reported data.

Computational methodology

All calculations were performed at the M06-2X level of theory with a mixed basis set using 6-31G(d) for C, H, N, and O and the LANL2DZ basis set for Co. Full geometry optimizations were carried out. The structures were modeled as neutral doublets (*i.e.* a single unpaired electron) with unrestricted calculations done for each structure. All calculations were done using Gaussian 09, revision B.01.

Results and discussion

New Co-Schiff base complexes **17a–f** were prepared in 6 synthetic steps from inexpensive, commercially available 2,3-dibromopropanol **8** (Scheme 1). Compound **8** was treated with an excess of sodium azide in dry DMF to afford a 90 : 10 mixture of diazidopropanol **9** and elimination product **10**. Substitution of alkyl bromides with azide is normally reported using water or absolute ethanol as solvent, but under those conditions, we instead observed rapid formation of symmetrical 1,3-diazidopropan-2-ol as the primary product *via* intermediate 1-bromo-2,3-epoxypropane.[23] Reduction of **9** to 2,3-diaminopropanol **11** was carried out using Staudinger conditions in the presence of triphenylphosphine.[24] Compound **11** was condensed with aldehyde **12** to afford unsymmetrical Schiff base **13** in 41% yield over three steps. To the best of our knowledge, the only reported preparation of such 2,3-diaminopropanol-based salen structures requires multiple steps starting from costly 2,3-diaminopropionic acid.[25]

Activation of the hydroxymethyl group in **13** toward direct nucleophilic introduction of a substituted piperazine under Mitsunobu conditions was unsuccessful and led instead to elimination product **13b**.[26] However, the primary hydroxyl group in **13** was activated toward nucleophilic attack *via* Steglich esterification[27] of **13** to smoothly provide ester **13a**, or *via* mesylation of **13** using standard procedures to give **14** in high yield. Compound **14** proved most useful for preparation of salen ligands **16**, as nucleophilic substitution with monosubstituted piperazines **15** in presence of DIPEA gave **16** in high yield. The use of DIPEA was crucial as it prevented quaternization of the piperazine moiety.[28] Other bases such as K$_2$CO$_3$, triethylamine or sodium hydride failed to yield the desired product. Attempted substitution at the mesyl group using other anionic species (*e.g.*, alkoxides) was also unsuccessful and led to **13b**. Finally, standard treatment of **16** with Co(OAc)$_2$·4H$_2$O in MeOH at reflux gave Co-Schiff base complexes **17a–f** in high yield.

Co-Schiff base complexes **17a–d** (5 mol%) catalyzed oxidation of syringyl alcohol **18** and vanillyl alcohol **19** (50 psi O$_2$, MeOH) as models of primary S and G units in lignin to *para*-benzoquinones **4** and **5** (Table 1). Catalysts **17a–d** gave conver-
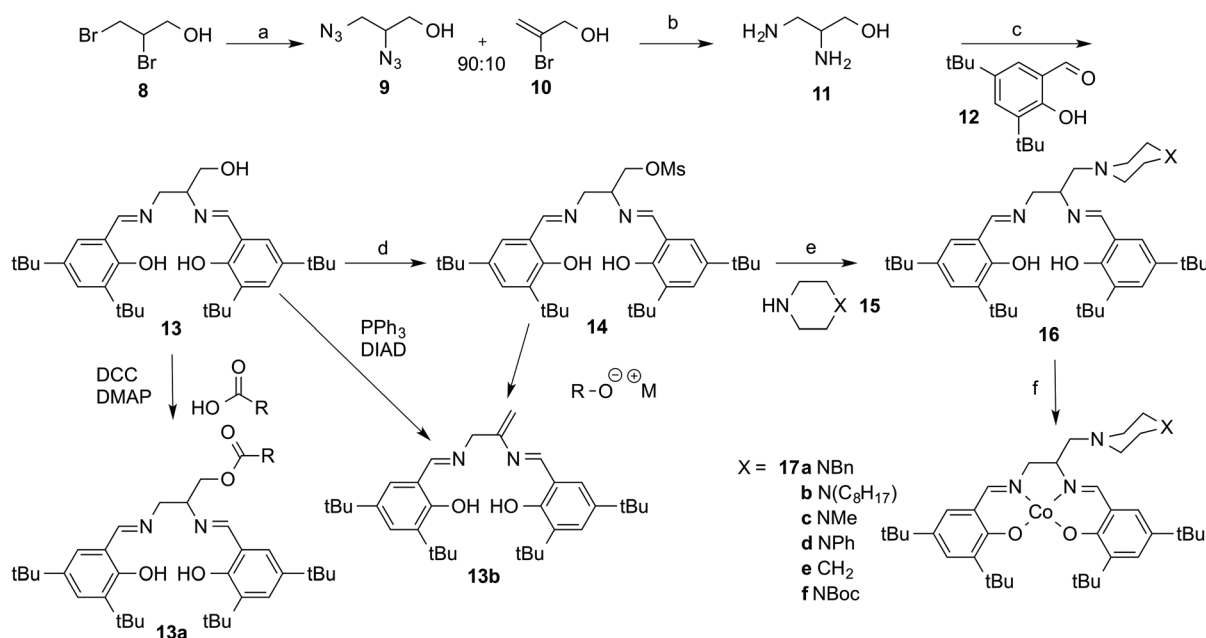
Scheme 1 Co-Schiff base complex synthesis. Reagents and conditions: (a) NaN$_3$, DMF, 70 °C, 16 h; (b) Ph$_3$P, THF–H$_2$O, reflux, 5 h; (c) 12, MeOH, reflux, 1 h (41%, 3 steps); (d) MsCl, Et$_3$N, CH$_2$Cl$_2$, rt, 1 h (95%); (e) 15, DIPEA, MeCN, reflux, 16 h (65–85%); (f) Co(OAc)$_2$·4H$_2$O, MeOH, reflux, 3 h (73–91%).

Table 1 Catalytic oxidation of **18** and **19** with Co-Schiff base complexes **17a–d**

Entry	Substrate	Catalyst	4/5[a] (%)	20/21[a] (%)	18/19[a] (%)	Entry	Substrate	Catalyst	4/5[a] (%)	20/21[a] (%)	18/19[a] (%)
1	**18**	**17a**	71	11	—	8	**19**	**17a**	72	5	—
2		**17b**	67	25	—	9		**17b**	68	—	10
3		**17b**[b]	Traces	Traces	>90						
4		**17c**	41	31	18	10		**17c**	59	22	—
5		**17d**	51	33	10	11		**17d**	54	15	Traces
6		**22**[c,d]	69	23	Traces	12		**22**[c,d]	56	Traces	—
7		**22**[c]	76	7	Traces	13		**22**[c]	46	Traces	38

[a] Yields are given for isolated materials. [b] 100% pyridine was added to the reaction. [c] 10 mol% of catalyst used. [d] 100% DIPEA was added to the reaction.

sions between 72–92% for **18** and 68–81% for **19**, affording DMBQ **4** and MMBQ **5** as primary products. Aldehydes **20** and **21** were observed as side products along with unreacted starting material. As was observed with structurally related catalysts such as **7**, an external axial base was not required in these oxidations. Indeed, addition of excess pyridine to an oxidation using catalyst **17b** completely inhibited the reaction resulting in recovery of the starting phenol (entry 3). However, the overall reactivity of these catalysts was lower than complex **7**, as evidenced by longer reaction times and somewhat lower yields. Qualitatively, reaction monitoring by TLC revealed a slower consumption of both **18** and **19**, and for **18** specifically, precipitation of DMBQ **4**, which has only limited solubility in the MeOH solvent, was slower over the course of the reaction.

Catalysts bearing sterically demanding and more highly basic groups such as **17a** and **17b** gave good yields of both **4** and **5**, accompanied by 5–25% benzaldehydes **20** and **21** (entries 1, 2, 8 and 9). Conversely, complexes with lower basicity at the substituent (**17d**) or those with reduced steric bulk (**17c**) gave a lower yield of quinone and higher levels of aldehyde (entries 4, 5, 10 and 11). Interestingly, the piperazinyl substituents appear to have a greater positive impact on the oxidation of G model **19** than S model **18**. Yields of **5** are about the same or slightly higher than **4** for reactions using catalysts **17a–d**, which is in contrast to oxidations catalyzed by simpler complexes, such as **1**.[17] In our previous work, catalyst **7** exhibited similar behavior, affording a 74% yield of **4** and an 83% yield of **5** from **18** and **19**, respectively.[19]

We further compared the reactivity of **17a–d** to catalyst **22**, which retains many of the steric features of the new catalysts but does not bear a hindered base as a substituent (entries 6, 7, 12 and 13). Although the reactivity of **22** is lower (10% catalyst is used), the absence of the basic substituent renders the complex considerably more effective in converting S models to **4** than G models into **5**. But consistent with earlier work,[18] the

ability of **22** to convert G models to MMBQ shows modest improvement when the oxidation is carried out in the presence of DIPEA (entry 12). Under the same conditions, the yield of **4** is slightly decreased (entry 6). The results in Table 1 demonstrate that including a bulky aliphatic base as a substituent on the Schiff-base ligand has a marked effect on the reactivity of the catalyst in promoting oxidation of *para*-substituted S and G lignin models. Moreover, the location of the hindered base with respect to the Co center affects the rate and yield of the reaction.

Computational analysis (DFT: M06-2X with the LANL2DZ basis set on the cobalt and 6-31G(d) basis set for all other elements) was used to examine these reactivity differences by comparing different conformations of catalyst **17a** (Fig. 3).

The *exo* conformation reduces crowding around the Co, but is calculated to be 11.24 kcal *less* stable than the conformation placing the substituent *endo* to the Co. In the *endo* conformation, the piperazine nitrogen closest to the Schiff base ligand restricts access to the Co, but is also is within coordination distance (2.45 Å), which stabilizes the complex. Similar intramolecular binding has been observed for Co-Schiff base complexes such as **23** bearing an alkoxymethyl group in the same position as the piperazine substituent in **17a**.[25] The increased crowding around the Co resulting from this intramolecular coordination may contribute to the diminished reactivity observed with catalysts such as **17a** when compared to more active catalysts such as **7** as formation of superoxo intermediate **2** (Fig. 1) could be slowed. This observation is also consistent with suppression of the oxidation using catalyst **17b** in the presence of excess pyridine, as the pyridine would occupy the remaining axial site on the Co and prevent binding of O₂ to form **2** (Table 1, entry 3).

The steric environment about the metal for these complexes may also be compared with Jacobsen's Mn-Schiff base asymmetric epoxidation catalysts, which employ the same
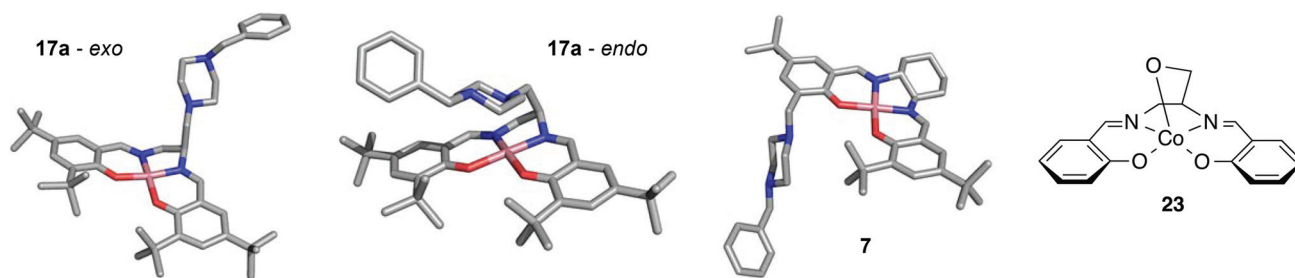
Fig. 3 Low energy conformations of complexes **17a** (*exo* and *endo*) and **7** (hydrogens omitted for clarity).

ligand as **22** and possess a steric barrier at their periphery as a result of the array of *t*-Bu groups. In these catalysts, the preferred trajectory for approach of a substrate to the central metal is across the face of the ligand's cyclohexyl group.[29] The *endo* conformation of catalysts **17a–d** places a substituent along this trajectory, resulting in a reduction of the catalyst's reactivity.

Comparative DFT evaluation of the more reactive catalyst **7** supports this hypothesis as its low energy conformation, in contrast to **17a**, places the piperazine nitrogens well outside of bonding distance to the Co. Examination of several alternate (and higher energy) conformations of **7** gives a calculated Co–N distance no less than 4.8 Å. Complex **7** thus retains steric features similar to Jacobsen's catalyst that would not significantly affect access to the Co.

The computational results also support the mechanistic scheme in Fig. 2. The ability of catalysts **17a–d** to oxidize both S and G lignin models is critical to their eventual utility for conversion of biorefinery lignin. The improved oxidation of G models that results by incorporating a hindered base within the catalyst structure may result from deprotonating the substrate in close proximity to the intermediate Co-superoxo linkage. This deprotonation enhances formation of the reactive phenoxy radical from the resulting phenoxide anion and would not be affected by intramolecular coordination in catalysts **17a–d** as the piperazine contains two basic centers. To test this hypothesis, we synthesized complexes **17e** and **17f**. By replacing the piperazine ligand with a piperidine group in **17e** and capping the non-binding nitrogen of the piperazine with a Boc group in **17f**, the second basic center in the substituent is removed. Both complexes exhibit a dramatically lower yield for the oxidation of **19** to **21** (Table 2).

Table 2 Oxidation using Co-Schiff base catalysts **17e** and **17f**

Substrate	Catalyst	4/5[a,b] (%)	20/21[a] (%)	18/19[a] (%)
18	**17e**	42	7	45
	17f	45	12	21
19	**17e**	16	—	79
	17f	13	—	65

[a] Yields are given for isolated materials. [b] Reaction conditions: 5 mol% catalyst, MeOH, O$_2$ (50 psi) rt, 16 h.

Such deprotonation may play a lesser role with S models. The presence of an additional OMe group on the aromatic ring can increase the rate of hydrogen atom removal by more than 100×,[17,30] leading to a much more facile formation of phenoxy radicals from S models by direct hydrogen atom removal by the Co-superoxo complex **2**. Thus, increased crowding of the coordination environment around the Co may affect loss of the hydrogen atom, which is reflected in the lower oxidation yields. Nonetheless, because the pK_a values for **18** and **19** are almost identical (9.87 and 9.78),[31] either substrate should undergo similar deprotonation, and the phenoxide derived from **18** may be contributing to the reaction.

Conclusions

Catalysts for lignin transformation will be most effective if designed to react with those functional groups present in highest concentration after lignin is isolated from renewable carbon sources. Our work is demonstrating that a focus on phenol oxidation, rather than β-aryl ether cleavage, is more representative of the actual functional group profile to be found in isolated, technical lignin. Further, the reactivity of these catalysts can be tuned by proper choice and position of sterically demanding groups within the structure of the ligand around the Co center. Incorporating a piperazinyl unit as part of the ligand increases the reactivity of the catalysts toward lignin G models without loss of reactivity toward S models. Our computational results also begin to clarify the mechanism of the process, and indicate how controlling access to the Co through ligation or steric crowding at the Co center can affect catalyst reactivity. These features will be critical in designing catalysts most effective for oxidation of all primary structural units in biorefinery lignin.

It is notable that these complexes induce oxidation in the absence of an added axial base, and that the addition of pyridine significantly inhibits quinone formation. Intramolecular coordination of the piperazine to the Co may activate binding to O$_2$ in a manner similar to complexes like Co(salpr) (**24**), particularly since computational results show such coordination

to be energetically favorable.

24
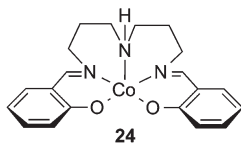
Related Co catalyzed oxidations have been reported that do not require added axial base.[32] However, these reactions are carried out under markedly different conditions in aqueous media and high pH, resulting in the presence of a high concentration of OH^- ions. The suggested mechanism is likely quite different from that occurring in nonaqueous media.[33] Moreover, the effectiveness of catalysts **7** and **22** suggest that coordination of an axial ligand may not be *required* for catalytic activity under these reaction conditions. In the case of **22**, our current results suggest that a non-coordinating aliphatic base is sufficient to promote formation of radical intermediate **3** and subsequent rearrangement to *para*-benzoquinones. The increased overall size of the Schiff base ligand in both **7** and **17a–d** may also be impeding catalyst deactivation pathways (such as formation of Co-peroxo dimers) that are easier with simpler complexes such as **1**. The impact of these various factors on the reaction mechanism and design of catalysts with higher reactivity and their use for oxidation of biorefinery lignin are under current active investigation.

Acknowledgements

Notes and references

1 J. J. Bozell, *Clean: Soil, Air, Water*, 2008, **36**, 641–647; J. J. Bozell and G. R. Petersen, *Green Chem.*, 2010, **12**, 539–554.

2 J. J. Bozell, J. E. Holladay, D. Johnson and J. F. White, *Top Value Added Chemicals from Biomass. Volume II – Results of Screening for Potential Candidates from Biorefinery Lignin*, Pacific Northwest National Laboratory, Richland, WA, 2007; J. Zakzeski, P. C. A. Bruijnincx, A. L. Jongerius and B. M. Weckhuysen, *Chem. Rev.*, 2010, **110**, 3552–3599; P. Sannigrahi, Y. Q. Pu and A. Ragauskas, *Curr. Opin. Environ. Sustainability*, 2010, **2**, 383–393.

3 W. Boerjan, J. Ralph and M. Baucher, *Ann. Rev. Plant Biol.*, 2003, **54**, 519–546.

4 A. U. Buranov and G. Mazza, *Ind. Crops Prod.*, 2008, **28**, 237–259.

5 N. Mosier, C. Wyman, B. Dale, R. Elander, Y. Y. Lee, M. Holtzapple and M. Ladisch, *Bioresour. Technol.*, 2005, **96**, 673–686.

6 D. Fengel and G. Wegener, *Wood. Chemistry, Ultrastructure Reactions*, Walter de Gruyter, Berlin, 1984.

7 A. Wu, B. O. Patrick, E. Chung and B. R. James, *Dalton Trans.*, 2012, **41**, 11093–11106; J. M. Nichols, L. M. Bishop, R. G. Bergman and J. A. Ellman, *J. Am. Chem. Soc.*, 2010, **132**, 12554–12555.

8 A. G. Sergeev and J. F. Hartwig, *Science*, 2011, **332**, 439–443; J. Y. He, C. Zhao and J. A. Lercher, *J. Am. Chem. Soc.*, 2012, **134**, 20768–20775.

9 T. H. Parsell, B. C. Owen, I. Klein, T. M. Jarrell, C. L. Marcum, L. J. Haupert, L. M. Amundson, H. I. Kenttamaa, F. Ribeiro, J. T. Miller and M. M. Abu-Omar, *Chem. Sci.*, 2013, **4**, 806–813.

10 J. Zakzeski, P. C. A. Bruijnincx and B. M. Weckhuysen, *Green Chem.*, 2011, **13**, 671–680.

11 S. K. Hanson, R. L. Wu and L. A. Silks, *Angew. Chem., Int. Ed.*, 2012, **51**, 3410–3413; S. Son and F. D. Toste, *Angew. Chem., Int. Ed.*, 2010, **49**, 3791–3794.

12 A. Rahimi, A. Azarpira, H. Kim, J. Ralph and S. S. Stahl, *J. Am. Chem. Soc.*, 2013, **135**, 6415–6418.

13 J. J. Bozell, C. J. O'Lenick and S. Warwick, *J. Agric. Food Chem.*, 2011, **59**, 9232–9242; J. B. Li, G. Gellerstedt and K. Toven, *Bioresour. Technol.*, 2009, **100**, 2556–2561; R. Samuel, Y. Q. Pu, B. Raman and A. J. Ragauskas, *Appl. Biochem. Biotechnol.*, 2010, **162**, 62–74.

14 Y. Z. Lai and X. P. Guo, *Wood Sci. Technol.*, 1991, **25**, 467–472.

15 A. Zombeck, R. S. Drago, B. B. Corden and J. H. Gaul, *J. Am. Chem. Soc.*, 1981, **103**, 7580–7585.

16 P. G. Cozzi, *Chem. Soc. Rev.*, 2004, **33**, 410–421; D. Chen, A. E. Martell and Y. Z. Sun, *Inorg. Chem.*, 1989, **28**, 2647–2652.

17 J. J. Bozell, B. R. Hames and D. R. Dimmel, *J. Org. Chem.*, 1995, **60**, 2398–2404.

18 D. Cedeno and J. J. Bozell, *Tetrahedron Lett.*, 2012, **53**, 2380–2383.

19 B. Biannic and J. J. Bozell, *Org. Lett.*, 2013, **15**, 2730–2733.

20 T. Elder, J. J. Bozell and D. Cedeno, *Phys. Chem. Chem. Phys.*, 2013, **15**, 7328–7337.

21 P. Hayes and C. Maignan, *Synthesis*, 1999, 783–786.

22 D. E. Bergbreiter, P. L. Osburn and C. M. Li, *Org. Lett.*, 2002, **4**, 737–740.

23 A. R. Kiasat, R. Badri, B. Zargar and S. Sayyahi, *J. Org. Chem.*, 2008, **73**, 8382–8385.

24 Y. G. Gololobov, I. N. Zhmurova and L. F. Kasukhin, *Tetrahedron*, 1981, **37**, 437–472.

25 R. Blaauw, J. L. van der Baan, S. Balt, M. W. G. de Bolster, G. W. Klumpp, H. Kooijman and A. L. Spek, *Inorg. Chim. Acta*, 2002, **336**, 29–38.

26 K. E. Elson, I. D. Jenkins and W. A. Loughlin, *Org. Biomol. Chem.*, 2003, **1**, 2958–2965.

27 B. Neises and W. Steglich, *Angew. Chem., Int. Ed. Engl.*, 1978, **17**, 522–524.

28 J. L. Moore, S. M. Taylor and V. A. Soloshonok, *ARKIVOC*, 2005, 287–292.

29 E. N. Jacobsen, W. Zhang, A. R. Muci, J. R. Ecker and L. Deng, *J. Am. Chem. Soc.*, 1991, **113**, 7063–7064; P. J. Pospisil, D. H. Carsten and E. N. Jacobsen, *Chem. – Eur. J.*, 1996, **2**, 974–980.

30 J. A. Howard and K. U. Ingold, *Can. J. Chem.*, 1963, **41**, 2800–2806; P. Mulder, O. W. Saastad and D. Griller, *J. Am. Chem. Soc.*, 1988, **110**, 4090–4092.

31 M. Ragnar, C. T. Lindgren and N. O. Nilvebrant, *J. Wood Chem. Technol.*, 2000, **20**, 277–305.

32 K. Kervinen, H. Kopi, M. Leskela and T. Repo, *J. Mol. Catal. A: Chem.*, 2003, **203**, 9–19.

33 K. Kervinen, H. Korpi, J. G. Mesu, F. Soulimani, T. Repo, B. Rieger, M. Leskela and B. M. Weckhuysen, *Eur. J. Inorg. Chem.*, 2005, 2591–2599.